REPORT DOCUMENTATION PAGE

Form Approved OMB NO. 0704-0188

1. REPORT DATE (DD-MM-YYYY)	2. REPORT TYPE	3. DATES COVERED (From - To)
04-05-2016	Final Report	20-Mar-2014 - 19-Mar-2016

4. TITLE AND SUBTITLE
Final Report: Instrumentation to Support the Development of New Nanomaterials for High Power Fiber Lasers

5a. CONTRACT NUMBER
W911NF-14-1-0134

5b. GRANT NUMBER

5c. PROGRAM ELEMENT NUMBER
206022

6. AUTHORS
Darayas N. Patel

5d. PROJECT NUMBER

5e. TASK NUMBER

5f. WORK UNIT NUMBER

7. PERFORMING ORGANIZATION NAMES AND ADDRESSES
Oakwood University
7000 Adventist Boulevard

Huntville, AL 35896 -0003

8. PERFORMING ORGANIZATION REPORT NUMBER

9. SPONSORING/MONITORING AGENCY NAME(S) AND ADDRESS (ES)
U.S. Army Research Office
P.O. Box 12211
Research Triangle Park, NC 27709-2211

10. SPONSOR/MONITOR'S ACRONYM(S)
ARO

11. SPONSOR/MONITOR'S REPORT NUMBER(S)
64757-PH-REP.1

12. DISTRIBUTION AVAILIBILITY STATEMENT
Approved for Public Release; Distribution Unlimited

13. SUPPLEMENTARY NOTES
The views, opinions and/or findings contained in this report are those of the author(s) and should not contrued as an official Department of the Army position, policy or decision, unless so designated by other documentation.

14. ABSTRACT
High average power fiber lasers and amplifiers have numerous industrial, scientific, and defense applications. Defense applications include laser-based weapons, laser-induced spark, and lidar. The small size and high optical-to-optical efficiency of fiber lasers and amplifiers also makes them promising components for scalable high-power laser systems employing spectral or coherent beam combination, but the output power and energy from individual fiber lasers have yet to reach their full potential. The main limitations for scaling fiber lasers and amplifiers to higher power and higher energy are nonlinear optical effects within the active gain fibers and thermal failure due to

15. SUBJECT TERMS
Nano-materials, fibers, spectrometer, radiometer, ball mill, Optical response, analuzer, fiber splicer, XRD system

16. SECURITY CLASSIFICATION OF:			17. LIMITATION OF ABSTRACT	15. NUMBER OF PAGES	19a. NAME OF RESPONSIBLE PERSON
a. REPORT	b. ABSTRACT	c. THIS PAGE			Darayas Patel
UU	UU	UU	UU		19b. TELEPHONE NUMBER 256-726-7558

Report Title

Final Report: Instrumentation to Support the Development of New Nanomaterials for High Power Fiber Lasers

ABSTRACT

High average power fiber lasers and amplifiers have numerous industrial, scientific, and defense applications. Defense applications include laser-based weapons, laser-induced spark, and lidar. The small size and high optical-to-optical efficiency of fiber lasers and amplifiers also makes them promising components for scalable high-power laser systems employing spectral or coherent beam combination, but the output power and energy from individual fiber lasers have yet to reach their full potential. The main limitations for scaling fiber lasers and amplifiers to higher power and higher energy are nonlinear optical effects within the active gain fibers and thermal failure due to extremely high power densities of the pump and laser radiation.

Enter List of papers submitted or published that acknowledge ARO support from the start of the project to the date of this printing. List the papers, including journal references, in the following categories:

(a) Papers published in peer-reviewed journals (N/A for none)

Received Paper

TOTAL:

Number of Papers published in peer-reviewed journals:

(b) Papers published in non-peer-reviewed journals (N/A for none)

Received Paper

TOTAL:

Number of Papers published in non peer-reviewed journals:

(c) Presentations

Submitted for publication

Abdalla Darwish, Abdul Aziz Muhammad, Deonte Alexander, Sergey Sarkisov, Darayas Patel, Paolo Mele, Brent Koplitz, Michael Johnson, Xiaodong Zhang, Polymer nano-composite films with inorganic upconversion phosphor and electro-optic additives made by concurrent triple-beam matrix assisted and direct pulsed laser deposition, submitted to Composites Part B.

Presentations
Poster presentation was presented by the PI and his student in San Francisco, CA, in Feb. 2014 at Photonics West 2014.
Poster presentation was presented by the PI and his student in San Francisco, CA, in Feb. 2015 at Photonics West 2015.

Number of Presentations: 1.00

Non Peer-Reviewed Conference Proceeding publications (other than abstracts):

Received Paper

TOTAL:

Number of Non Peer-Reviewed Conference Proceeding publications (other than abstracts):

Peer-Reviewed Conference Proceeding publications (other than abstracts):

Received Paper

TOTAL:

Number of Peer-Reviewed Conference Proceeding publications (other than abstracts):

(d) Manuscripts

Received Paper

TOTAL:

Number of Manuscripts:

Books

Received Book

TOTAL:

Received	Book Chapter

TOTAL:

Patents Submitted

Patents Awarded

Awards

Graduate Students

NAME	PERCENT_SUPPORTED

FTE Equivalent:
Total Number:

Names of Post Doctorates

NAME	PERCENT_SUPPORTED

FTE Equivalent:
Total Number:

Names of Faculty Supported

NAME	PERCENT_SUPPORTED

FTE Equivalent:
Total Number:

Names of Under Graduate students supported

NAME	PERCENT_SUPPORTED	Discipline
Ruben Valentine	0.00	Engineering Major, Senior
Donald M. Wright III	0.00	Engineering Major, Senior
Danielle Lewis	0.00	Engineering Major, Senior
Marcus Valentine	0.00	Engineering Major, Senior
FTE Equivalent:	**0.00**	
Total Number:	**4**	

Student Metrics

This section only applies to graduating undergraduates supported by this agreement in this reporting period

The number of undergraduates funded by this agreement who graduated during this period: 4.00

The number of undergraduates funded by this agreement who graduated during this period with a degree in science, mathematics, engineering, or technology fields:..... 3.00

The number of undergraduates funded by your agreement who graduated during this period and will continue to pursue a graduate or Ph.D. degree in science, mathematics, engineering, or technology fields:..... 3.00

Number of graduating undergraduates who achieved a 3.5 GPA to 4.0 (4.0 max scale):..... 0.00

Number of graduating undergraduates funded by a DoD funded Center of Excellence grant for Education, Research and Engineering:..... 0.00

The number of undergraduates funded by your agreement who graduated during this period and intend to work for the Department of Defense 0.00

The number of undergraduates funded by your agreement who graduated during this period and will receive scholarships or fellowships for further studies in science, mathematics, engineering or technology fields: 0.00

Names of Personnel receiving masters degrees

NAME
Total Number:

Names of personnel receiving PHDs

NAME
Total Number:

Names of other research staff

NAME	PERCENT_SUPPORTED
FTE Equivalent:	
Total Number:	

Sub Contractors (DD882)

Inventions (DD882)

Scientific Progress

Technology Transfer

FINAL TECHNICAL REPORT
FOR
DEPARTMENT OF DEFENSE

INSTRUMENTATION TO SUPPORT THE DEVELOPMENT OF NEW NANOMATERIALS FOR HIGH POWER FIBER LASERS

Proposal # 64757-RT-REP
Agreement # W911NF-14-1-0134

REPORTING PERIOD FROM MARCH 2014 TO APRIL 14 2016

Prepared by

Dr. Darayas Patel
Department of Mathematics & Computer Science
Oakwood University
Huntsville, AL 35896
Email: dpatel@oakwood.edu

Project summary

Significant accomplishments:

The following groups of have been acquired: (A) Inert Gas Purgeable Furnace EW-33854-15 (Cole-Palmer) and XRD system D2 Phaser (Bruker); (B) UV-VIS-NIR-IR Spectrophotometer system: Shimatzu 2600, Nicolet iS5 (Thermo Scientific), and Ava-Raman-785TEC-USB2 (Avantes); (C) PQ-N04 Planetary Ball Mill PQ-N04 (Across International); (D) Radiometer System: ISR-2600Plus two-detector integrating sphere (Shimatzu), Spectral radiometer GS-001X/ GS-002EX (SSSOT), Laser Power Meter FieldMaxII with Sensors (Coherent); (E) Analyzer of Optical Response AOR-001X/ AOR-002EX (SSSOT); (F) Optical Fiber Splicer System: Fujikura 12S+CT-30 and LFS-004 (SSSOT); (G) Optical Fiber Spectrum Analyzer MS9740A (Anritsu) and Digital Pulse Generator DG53502 (Stanford Research).

The acquired instrumentation has been critical in the completion of the research project "New nanomaterials for high power fiber lasers" sponsored by DoD through research Grant # **W911NF-14-1-0134** (from March 2014 to April 2016). The major accomplishments are the following:

1) The role of post-synthetic baking (with the help of the acquired furnace) of Rare Earth phosphor $NaYF_4$: Yb^{3+}, Er^{3+} was investigated in detail using the acquired XRD instrument. One-hour baking of the freshly synthesized powder within the temperature range between 400 and 600^{o}C lead to the transition from the cubic α-phase to the hexagonal β-phase of the host $NaYF_4$ that was favorable for the up- and downconversion emission of the phosphor being pumped with 980-nm radiation.

2) Optical properties of the synthesized laser material, such as the spectrum of the optical absorption bands and the quantum efficiency of the radiation, were investigated using the acquired spectroscopic and radiometric instrumentation. The synthesized phosphor had a strong absorption band around 977-nm suitable for pumping with a 980-nm laser diode. The quantum efficiency of upconversion radiation was measured to be 0.56% (of the same order of magnitude as the best reported in the literature).

3) The two-stage ball-milling process of pulverization of the phosphor micro-powder in a nanocolloid was developed and refined with the help of the ball milling instrument. Two-stage ball-milling with 5-mm and 0.5-mm Zirconia balls in Zirconia cups resulted in resulted in the nanoparticles of ~ 100-nm diameter.

4) A nanocolloid optical fiber amplifier was built using the acquired fusion fiber splicing instrumentation. Experimental setup was developed and tested for the investigation of nanocolloid optical fiber amplifiers and lasers using the acquired optical spectrum analyzer and pulse generator. All the major effects of the operation of the Erbium (three-level) based nanocolloid gain media were observed and verified by comparison with the literature data.

5) Additionally, the synthesized phosphor was explored as a basis for chemical sensors with the help of the instrumentation analyzing its optical response to air pollutants such as ammonia. The sensitivity of the experimental sensor was ~ 0.4% of ammonia with 5-min time response.

Future plans:

1) Further development of an efficient Rare Earth phosphor nano-material and building a prototype of a nanocolloid fiber amplifier/laser based on the synthesized material.

2) The development of the prototype of the chemical sensor of various air and water pollutants using the developed phosphor material and for chem- and bio-defense.

Figure captions

Figure 1. XRD spectrum of the synthesized powder of $NaYF_4$: Yb^{3+}, Er^{3+} at various baking temperature. 1 – the reference XRD spectrum (calculated line pattern – JCPDS card No. 77-2042) of $NaYF_4$ α –phase (cubic); 2 – XRD spectrum of the synthesized powder of $NaYF_4$: Yb^{3+}, Er^{3+} without baking; 3 - XRD spectrum of the synthesized powder of $NaYF_4$: Yb^{3+}, Er^{3+} baked for 1 hour at 300^{o}C; 4 - 400 ^{o}C; 5 - 500 ^{o}C; 6 - 600 ^{o}C; 7 - 700 ^{o}C; 8 - 800 ^{o}C; 9 – the reference XRD spectrum (calculated line pattern – JCPDS card No. 28-1192) of $NaYF_4$ β –phase (hexagonal).

Figure 2. Optical absorption spectrum of the $NaYF_4$: Er^{3+}, Yb^{3+} micro-powder taken with UV-VIS-NIR spectrophotometer Shimatzu 2600.

Figure 3. Size distribution of the nanocolloid of $NaYF_4$: Er^{3+}, Yb^{3+} in CCl_4 (ball-milled with 5-mm and 0.5-mm balls) obtained with the dynamic light scattering (DLS) measurement (Zetasizer 90). The nanocolloid was filtered through one-micron filter. Solid and dashed lines correspond to two sets of measurement data.

Figure 4. Block diagram of the experimental setup to measure the quantum efficiency of the RE phosphor (a) and the photograph of the integrating sphere and the Spectral Radiometer GS-001X/ GS-002EX of the Radiometer System (b).

Figure 5. Diagram explaining the principle of operation of the polymer composite film containing the developed RE phosphor as the sensor of ammonia.

Figure 6. Schematic of the experimental setup to investigate the RE phosphor impregnated films for sensing ammonia using the Analyzer of Optical Response AOR-001X/AOR-002EX.

Figure 7. Photograph of the experimental setup to investigate RE phosphor based films for chemical sensing with the major components of the Analyzer AOR-001X.

Figure 8. Top view of analyzer AOR-002EX with open cover.

Figure 9. Time plot of the response of the sample nano-composite RE based reagent film to the exposure to 5% ammonia in air.

Figure 10. Ammonia concentration plotted versus the sensor output. Solid line presents the approximation quadratic calibration curve.

Figure 11. Image of the nanocolloid optical fiber amplifier based on a hollow fiber filled with the nanocolloid of RE phosphor $NaYF_4$: Yb^{3+}, Er^{3+} in a high-index liquid. The bright trace of visible light is produced by the upconversion emission from the nanocolloid pumped with a 980-nm IR radiation entering the fiber from the left. The pump radiation is delivered via a 980/1550-nm single-mode optical fiber spliced to the hollow fiber using Optical Fiber Splicer System including Fujikura 12S+CT-30 fusion splicer and LFS-004 (SSSOT) splicer/integrity tester.

Figure 12. Experimental setup to characterize a nanocolloid fiber amplifier using Optical Fiber Spectrum Analyzer MS9740A (Anritsu) and Digital Pulse Generator DG53502 (Stanford Research).

Figure 13. Output pulsed signal (1550 nm) for pump power: 0 mw (1) and 4.0 mW (2).

Figure 14. Gain versus pump power for input signal: 0.05 mW (1); 0.1 mW (2); 0.15 mW (3).

Figure 15. Gain versus input signal for pump power: 129 mW (1); 217 mW.

Table of Contents

1. Introduction

High average power fiber lasers and amplifiers have numerous industrial, scientific, and defense applications. Defense applications include laser-based weapons, laser-induced spark, and lidar. The small size and high optical-to-optical efficiency of fiber lasers and amplifiers also makes them promising components for scalable high-power laser systems employing spectral or coherent beam combination, but the output power and energy from individual fiber lasers have yet to reach their full potential. The main limitations for scaling fiber lasers and amplifiers to higher power and higher energy are nonlinear optical effects within the active gain fibers and thermal failure due to extremely high power densities of the pump and laser radiation. In order to overcome the limitations Dr. D. Patel from Oakwood University, the PI, has been conducting research project "New nanomaterials for high power fiber lasers" sponsored by DoD through research Grant **W911NF-14-1-0134** (from March 2014 to April 2016). The goal of this instrumentation project was to support the research efforts of Dr. Patel with the necessary research instrumentation and improve the capabilities of the Oakwood University in the direction of new laser nanomaterials and nanophotonics related to the DoD needs.

2. Significant accomplishments

This section describes the acquired instrumentation and the major research results obtained with it. The results are relevant to the research effort of Dr. Patel in the direction of new nanomaterials for high power fiber amplifiers and lasers.

2.1. Inert Gas Purgeable Furnace EW-33854-15 (Cole-Palmer) and XRD system D2 Phaser (Bruker)

As a source material for the laser nanocolloid medium was chosen the Rare Earth (RE)-doped compound $NaYF_4$: Yb^{3+}, Er^{3+}. The rationale behind this choice is the following. The efficiency of conversion of the energy of pump radiation (usually from a 980-nm laser diode) to the laser radiation greatly depends on the host for the RE ions. Popular modern highly efficient RE based laser materials use hexagonal-phase crystalline $NaYF_4$ (β-$NaYF_4$) as the host material due to the low phonon energy of the crystal lattice that minimizes the non-radiative multi-phonon relaxation process of the excited RE dopants. The three-valent ion of Yb acts as a "synthesizer" absorbing the photon of a 980-nm pump radiation. Then it radiationlessly transfers the energy to the ion of Er that produces the downconversion emission at 1550-nm (conventional laser line) and upconversion visible emission.

The micro-powder of $NaYF_4$: Yb^{3+}, Er^{3+} was synthesized using a simple solution based technique (wet process) in the presence of Na_2-ethylenediaminetetraacetic acid (EDTA) with the co-precipitation procedure to obtain homogeneous nucleation.

The freshly made RE phosphor powder did not exhibit any noticeable up- or downconversion emission. Inert Gas Purgeable Furnace EW-33854-15 was used to bake the synthesized RE phosphor micro-powder to convert it in the hexagonal-phase crystalline $NaYF_4$ (β-$NaYF_4$) favorable for up- or downconversion emission. XRD system D2 Phaser was used to analyze the crystalline structure of the phosphor at different baking temperatures. Figure 1 presents the X-ray

diffraction spectra of the synthesized micro-powder of $NaYF_4$:Yb^{3+}, Er^{3+} baked after preparation for one hour at different temperatures in comparison with the reference cubic α-phase $NaYF_4$ and hexagonal β-phase $NaYF_4$. With the increase of the baking temperature from "no-baking" to 300^{o}C the powder remains to be in the α -NaYF4 (cubic) phase. Starting from 400^{o}C, the β - NaYF4 (hexagonal) phase is dominating. After 700^{o}C, the β - NaYF4 (hexagonal) phase is replaced back by the α -NaYF4 (cubic) phase. It thus could be concluded that the most favorable for good up- and downconversion efficiency (and laser/amplifier use) of the phosphor would be a baking temperature between 400 and 700^{o}C.

2.2. UV-VIS-NIR-IR Spectrophotometer system: Shimatzu 2600, Nicolet iS5 (Thermo Scientific), and Ava-Raman-785TEC-USB2 (Avantes)

The optical absorption NIR spectrum of the RE-based phosphor $NaYF_4$: Yb^{3+}, Er^{3+} was measured with UV-VIS-NIR spectrophotometer Shimatzu 2600. It is presented in Fig. 2. The strong absorption peak near 980 nm can be attributed to the three-valent ion of Yb. This result indicated that a 980-nm laser diode can be effectively used as a pump source for the amplifier/laser action of the phosphor-based gain medium.

2.3. PQ-N04 Planetary Ball Mill PQ-N04 (Across International)

The RE phosphor powder was pulverized into nanocolloids using the ball milling process with a PQ-N04 Planetary Ball Mill from Across International. 50-ml Zirconia cups and Zirconia balls (5-mm and 0.5-mm diameter were used. Ball milling was done in water three times with each set of balls. The cups were loaded with the balls to the 2/3 of volume. 20 ml of the liquid was added in the cup and from 1 or 2 g of the micro-powder. Alternating directions of rotation were chosen during the milling with 5-min duration of the rotation in one direction and 10-min pause between rotations (for cooling). Number of operation and re-starting times was 20. Total duration of the rotation during a single process thus was 1 h 40 min**.** After ball-milling the colloid was transferred with a pipette from the cup in a tube. One drop of oleic acid (surfactant to prevent clustering of the nanoparticles) was added. The colloid was sonicated in an ultrasonic bath for 60 min. Then it was left to precipitate for several hours and dry. Afterwards, it could be transferred to different liquids. Finally, it was filtered with a 1-micron filter. Figure 3 presents the size distribution of the nanocolloid in CCl_4 measured with a dynamic light scatterometer. The measurement was performed two times (solid and dashed lines in Fig. 3). The nanocolloid consists of two species of nanoparticles. The dominant group is made of nanoparticles with a size of approximately 122 nm.

2.4. Radiometer System: ISR-2600Plus two-detector integrating sphere (Shimatzu), Spectral radiometer GS-001X/ GS-002EX (SSSOT), Laser Power Meter FieldMaxII with Sensors (Coherent).

The Radiometer System (Fig. 4) was used to measure the quantum efficiency (QE) of the emission of the RE micro- and nano-powders was estimated using the following approach. QE could be defined as the ratio of the number of the photons of the up- or downconversion (as an example, the upconversion is considered) radiation generated per unit of time n_{up} to the number of the photons of the infra-red pump radiation n_{pump}

$$\eta = \frac{n_{up}}{n_{pump}} 100\% \ .$$

QE of the upconversion emission was measured to be

$$\eta = \frac{P_{up\,tot}\lambda_{up}}{P_{pump\,tot}\lambda_{pump}} 100\% = 0.56\% \ ,$$

where P_{up} was the measured power of the upconversion emission (at 540 nm); λ_{up} was the wavelength of the upconversion emission (~ 540 nm); P_{pump} was the power of the pump; λ_{pump} was the wavelength of the pump radiation (980 nm). The computed value compared well against 3% QE reported for similar upconversion phosphor $NaYF_4$: Yb^{3+}, Er^{3+} in Ref. 1.

2.5. Analyzer of Optical Response AOR-001X/ AOR-002EX (SSSOT)

The Analyzer of Optical Response was used to explore the application of the developed RE phosphor to chemical sensors, particularly sensors of ammonia. The principle of functioning of the ammonia sensor under consideration is illustrated in Fig. 5. A polymer nano-composite film containing RE phosphor is additionally doped with an indicator dye (Phenol Red), which turns from yellow to red upon exposure to atmospheric ammonia. The upconversion phosphor nano-particulate of the film is illuminated with an infra-red laser diode (980 nm wavelength) and generates upconversion visible light of green color (~ 540 nm spectral peak). When the indicator dye exposed to ammonia turns red, it absorbs the green light from the phosphor: higher concentration of ammonia corresponds to the weaker intensity of the green light recorded by a photodetector.

The prepared reagent nano-composite films were tested as ammonia sensors using the experimental setup using Analyzer AOR-001X/AOR-002EX schematically depicted in Fig. 6. The photographs of the general view of AOR-001X and AOR-002EX are presented in Figs. 7 and 8.

The reagent film deposited onto a silicon substrate (Sample) was placed inside a sealed gas chamber of AOR-001X. It was illuminated with a 980-nm radiation from a 300-mW laser diode. The radiation was delivered from the laser diode via a single-mode optical fiber terminated with a collimator. The collimated infra-red beam was sent to the film through a transparent plastic lid of the chamber. The green component of the upconversion radiation from the film passed through the transparent lid and got collected by the focusing optics that sent it though a multimode fiber to a silicon photodetector. The signal from the photodetector was digitized in a power meter module and sent to a computerized data acquisition and processing system. “Gas supply” was comprised of a mixture of ammonia and ambient air drawn through a water bubbler and further in the gas chamber with a vacuum pump.

The nano-composite reagent films were exposed to ammonia using the above-mentioned setup. Fig. 9 presents a typical response (the drop of the intensity of the green upconversion emission recorded with a power meter using a silicon photodetector) to ammonia (~5% molar concentration of ammonia in air). The relative humidity (RH) of the air during the exposure was ~ 50%. The film response to ammonia was not significantly affected by the variation of RH between 30 and almost 100%. Typical response time to the exposure was ~ 5 min.

Figure 10 presents a typical calibration plot "Ammonia concentration vs. Sensor Output". The absolute value of the drop of the power of the upconversion emission $-\Delta P$ (in nanoWatts) from the exposed reagent film was chosen as the sensor output. The plot is nonlinear and can be approximated with a quadratic curve (solid line). The nonlinearity of the response is typical for colorimetric sensors [2] and is an advantage when dealing with very wide range of possible exposure (from zero to high concentrations of NH_3). The reagent film has the capability of recovering from the exposure to very high ammonia concentrations without experiencing any irreversible damage. Based on the level of the fluctuations of the output readings, the sensitivity of the sensor could be estimated as ~ 0.4% of ammonia in air or 8% of the range 0 to 5% ammonia.

2.6. Optical Fiber Splicer System: Fujikura 12S+CT-30 and LFS-004 (SSSOT)

The Optical Fiber Splicer System including fusion splicer Fujikura 12S+CT-30 and splicer/integrity tester LFS-004 (SSSOT) was used to splice a 980/1550-nm single-mode optical fiber delivering 980-nm pump radiation to an optical fiber amplifier. The amplifier is based on a hollow fiber (SGE fused silica tubing; 0.15-mm inner diameter; 0.363-mm outer diameter) filled with the nanocolloid of RE phosphor $NaYF_4$: Yb^{3+}, Er^{3+} in a high-index liquid 1057B from Cargille Laboratories (Fig. 11). The bright trace of visible light is the upconversion emission from the nanocolloid filler pumped with the 980-nm radiation entering the fiber from the left.

2.7. Optical Fiber Spectrum Analyzer MS9740A (Anritsu) and Digital Pulse Generator DG53502 (Stanford Research)

Optical Fiber Spectrum Analyzer MS9740A (Anritsu) and Digital Pulse Generator DG53502 (Stanford Research) were used to characterize the optical fiber amplifier (described above) in the setup presented in Fig. 12. The input signal from a 1550-nm laser was modulated with Digital Pulse Generator DG53502. The signal and the pump radiation from a 980-nm laser diode were combined with a wave division multiplexer (WDM) and sent through the nanocolloid fiber amplifier. The output mixture of the amplified signal and the residual pump was sent via a multi-mode selfoc fiber to Optical Fiber Spectrum Analyzer MS9740A (when the pulse generator was turned off) or to an InGaAs photodetector connected to an oscilloscope. Pulse modulation was necessary to separate the signal from the continuous pump or the spontaneous emission created by the pump. The effective gain of the amplifier was computed using equation

$$Gain\ [dB] = 10log\left(\frac{Sign-out}{Sign-in}\right),$$

Where *Sign-in* and *Sign-out* is the power of the output signal with zero and non-zero pump power respectively. Figure 13 presents the output pulsed signal (at 1550 nm) for pump power 4.0 mW against the output signal with zero pump. The amplitude of the signal is amplified 5.4 times (Gain ≈ 7.3 dB). Figure 14 presents the gain measured with Optical Fiber Spectrum Analyzer MS9740A plotted versus the pump power for different powers of the input signal for the 7.0-cm-long nanocolloid fiber amplifier. The gain initially increases linearly with pump power, but then flattens out. Such behavior is expected since a large pump power will result in severe depletion of the ground state leading to reduced absorption and pumping rate. This phenomenon, referred to as pump saturation, prevails in all three-level systems (such as Erbium) where the lower gain

state is the ground state, which by definition must be at least 50% depleted simply to obtain a population inversion [3]. Figure 15 presents the gain plotted versus the input signal at different pump powers. One can see that at a given pump power the gain falls off as the system experiences the phenomenon referred to as gain saturation [3]. This arises from significant depletion of the upper state population by the high rate of the simulated emission. The saturated output power of the amplifier is that for which the gain has fallen by 3 dB with respect to the small signal gain.

2.8. Conclusions

The acquired instrumentation has been critical in the completion of the research project "New nanomaterials for high power fiber lasers" sponsored by DoD through research Grant **W911NF-14-1-0134** (from March 2014 to April 2016). The major accomplishments are the following:

6) The role of post-synthetic baking (with the help of the acquired furnace) of Rare Earth phosphor $NaYF_4$: Yb^{3+}, Er^{3+} was investigated in detail using the acquired XRD instrument. One-hour baking of the freshly synthesized powder within the temperature range between 400 and 600^{o}C lead to the transition from the cubic α-phase to the hexagonal β-phase of the host $NaYF_4$ that was favorable for the up- and downconversion emission of the phosphor being pumped with 980-nm radiation.
7) Optical properties of the synthesized laser material, such as the spectrum of the optical absorption bands and the quantum efficiency of the radiation, were investigated using the acquired spectroscopic and radiometric instrumentation. The synthesized phosphor had a strong absorption band around 977-nm suitable for pumping with a 980-nm laser diode. The quantum efficiency of upconversion radiation was measured to be 0.56% (of the same order of magnitude as the best reported in the literature).
8) The two-stage ball-milling process of pulverization of the phosphor micro-powder in a nanocolloid was developed and refined with the help of the ball milling instrument. Two-stage ball-milling with 5-mm and 0.5-mm Zirconia balls in Zirconia cups resulted in resulted in the nanoparticles of ~ 100-nm diameter.
9) A nanocolloid optical fiber amplifier was built using the acquired fusion fiber splicing instrumentation. Experimental setup was developed and tested for the investigation of nanocolloid optical fiber amplifiers and lasers using the acquired optical spectrum analyzer and pulse generator. All the major effects of the operation of the Erbium (three-level) based nanocolloid gain media were observed and verified by comparison with the literature data.
10) Additionally, the synthesized phosphor was explored as a basis for chemical sensors with the help of the instrumentation analyzing its optical response to air pollutants such as ammonia. The sensitivity of the experimental sensor was ~ 0.4% of ammonia with 5-min time response.

3. Future plans

The acquired instrumentation has significantly improved the capabilities of Oakwood University to conduct high level sponsored research related to the needs of DoD and other government agencies. Two particular directions of the future use of the acquired instrumentation are:

3) Further development of an efficient Rare Earth phosphor nano-material and building a prototype of a nanocolloid fiber amplifier/laser based on the synthesized material.

4) The development of the prototype of the chemical sensor of various air and water pollutants using the developed phosphor material and for chem- and bio-defense.

4. References

1. J.-Ch. Boyer and F.C. J. M. van Veggel, Absolute quantum yield measurements of colloidal $NaYF_4$: Er^{3+}, Yb^{3+} upconverting nanoparticles, Nanoscale 2 (2010) 1417-1419.
2. S. S. Sarkisov, M. Czarick III, B. D. Fairchild, Yi Liang, T. Kukhtareva, M. J. Curley, Colorimetric polymer-metal nanocomposite sensor of ammonia for the agricultural industry of confined animal feeding operations, Opt. Eng., vol. 53 (2), pp. 021107-1 - 021107-10, Feb. 2014.
3. P.C. Becker, N.A. Olsson, and J.R. Simpson, Erbium-doped fiber amplifiers: Fundamentals and Technology, Academic Press, San Diego, 1997.

5. Figures

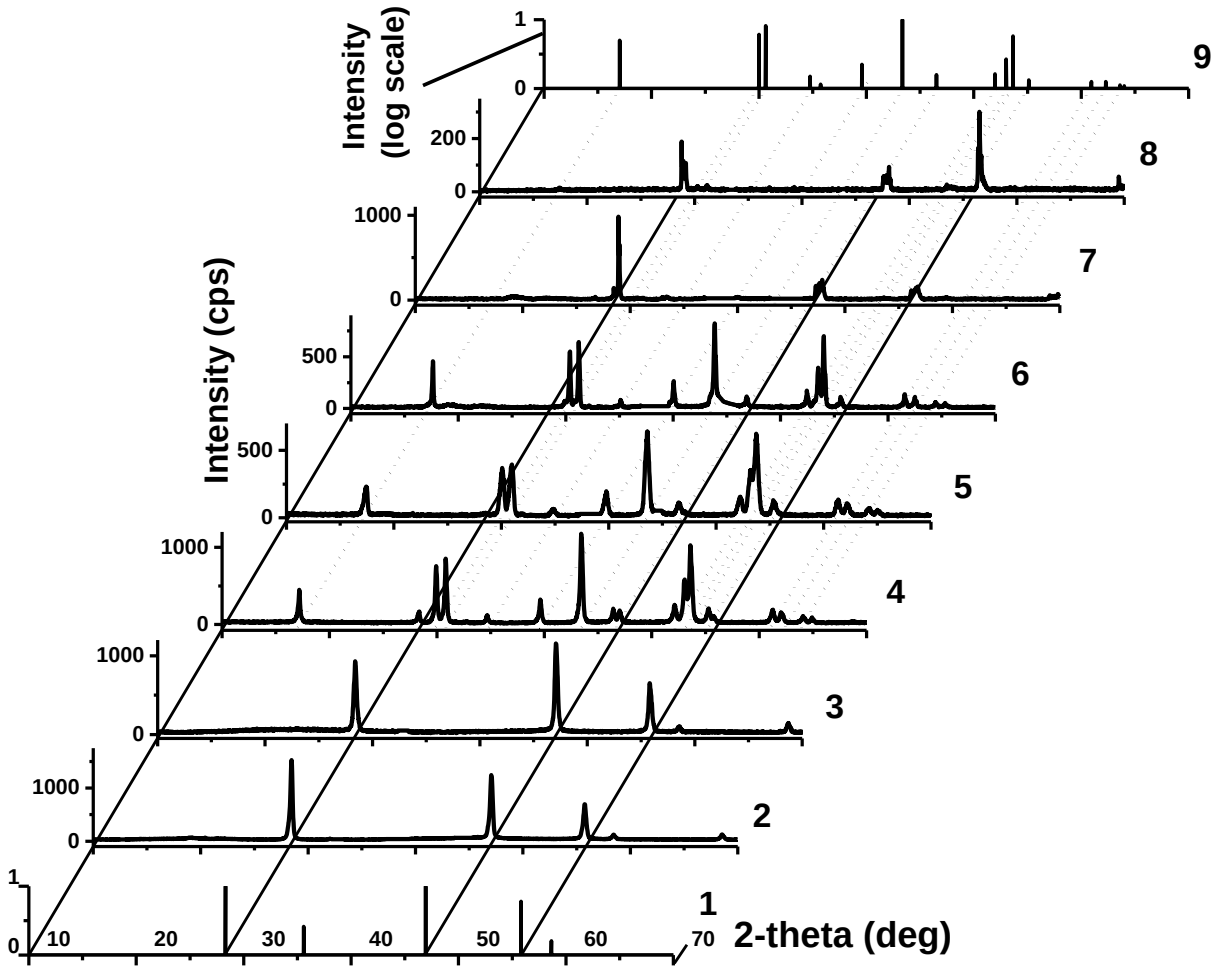

Figure 1. XRD spectrum of the synthesized powder of $NaYF_4$: Yb^{3+}, Er^{3+} at various baking temperature. 1 – the reference XRD spectrum (calculated line pattern – JCPDS card No. 77-2042) of $NaYF_4$ α –phase (cubic); 2 – XRD spectrum of the synthesized powder of $NaYF_4$: Yb^{3+}, Er^{3+} without baking; 3 - XRD spectrum of the synthesized powder of $NaYF_4$: Yb^{3+}, Er^{3+} baked for 1 hour at 300^{o}C; 4 - 400 ^{o}C; 5 - 500 ^{o}C; 6 - 600 ^{o}C; 7 - 700 ^{o}C; 8 - 800 ^{o}C; 9 – the reference XRD spectrum (calculated line pattern – JCPDS card No. 28-1192) of $NaYF_4$ β –phase (hexagonal).

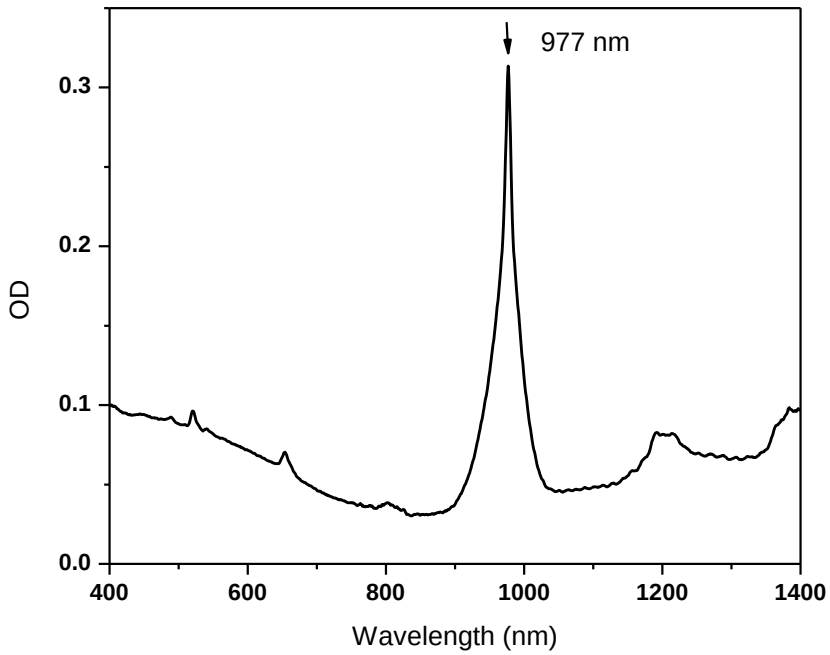

Figure 2. Optical absorption spectrum of the $NaYF_4$: Er^{3+}, Yb^{3+} micro-powder taken with UV-VIS-NIR spectrophotometer Shimatzu 2600.

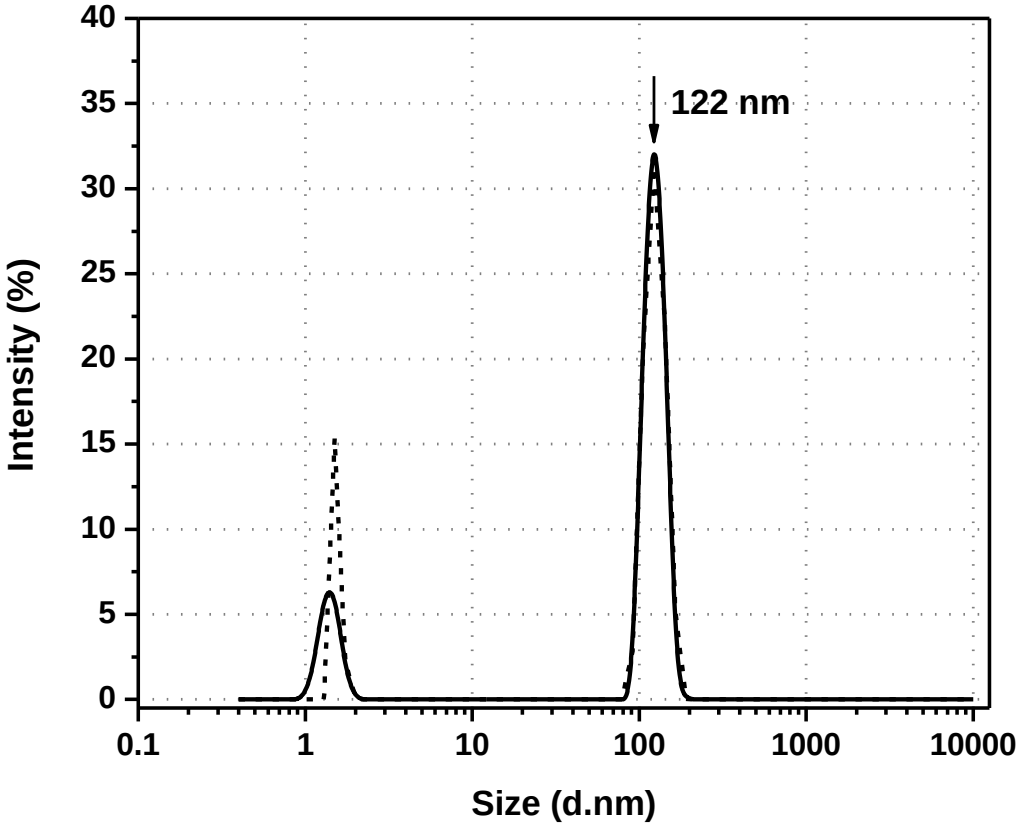

Figure 3. Size distribution of the nanocolloid of $NaYF_4$: Er^{3+}, Yb^{3+} in CCl_4 (ball-milled with 5-mm and 0.5-mm balls) obtained with the dynamic light scattering (DLS) measurement (Zetasizer 90). The nanocolloid was filtered through one-micron filter. Solid and dashed lines correspond to two sets of measurement data.

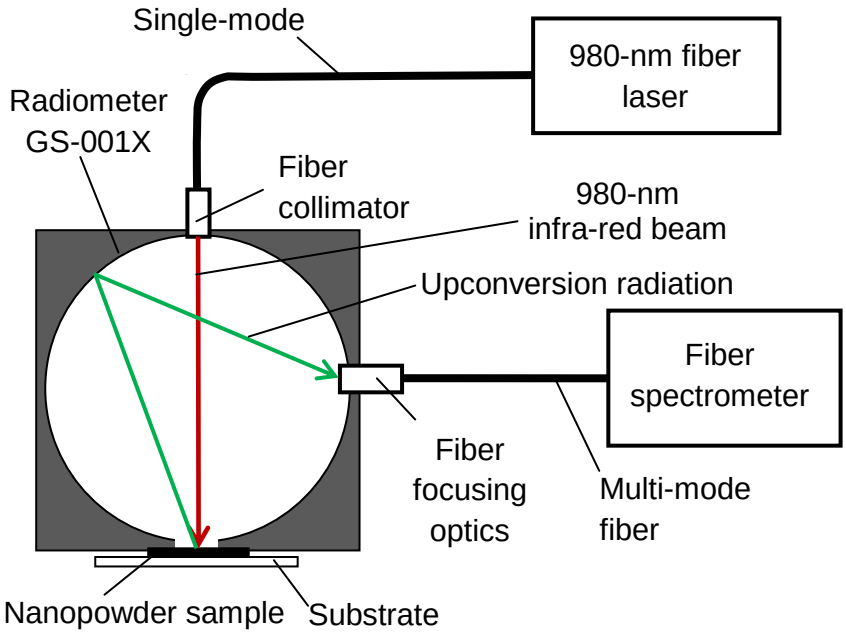

(a)

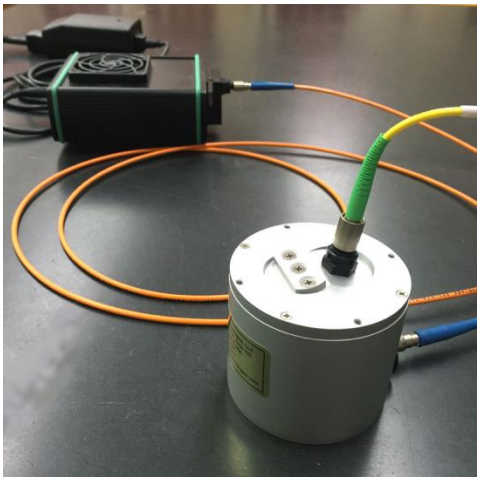

(b)

Figure 4. Block diagram of the experimental setup to measure the quantum efficiency of the RE phosphor (a) and the photograph of the integrating sphere and the Spectral Radiometer GS-001X/ GS-002EX of the Radiometer System (b).

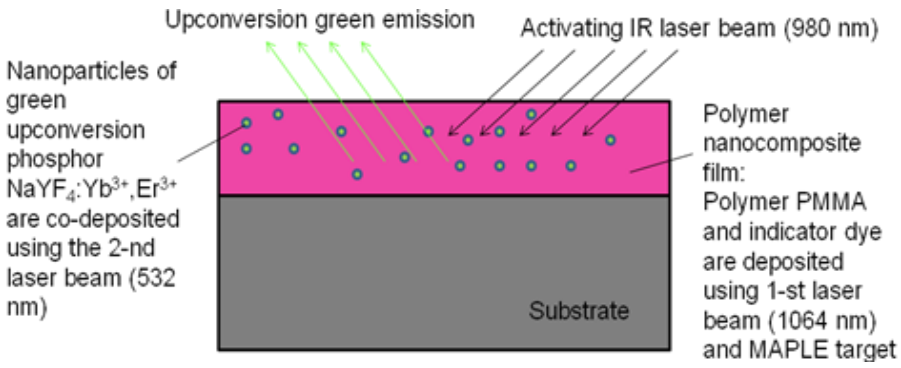

Figure 5. Diagram explaining the principle of operation of the polymer composite film containing the developed RE phosphor as the sensor of ammonia.

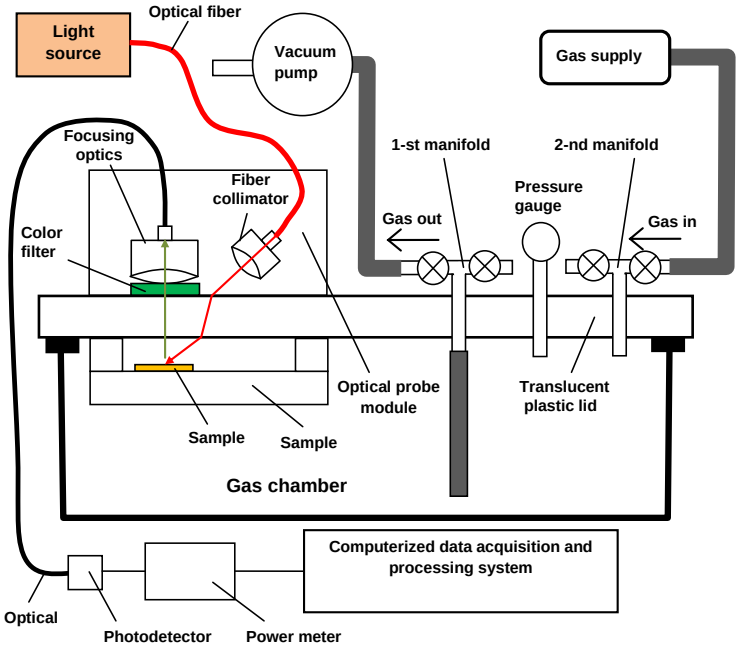

Figure 6. Schematic of the experimental setup to investigate the RE phosphor impregnated films for sensing ammonia using the Analyzer of Optical Response AOR-001X/AOR-002EX.

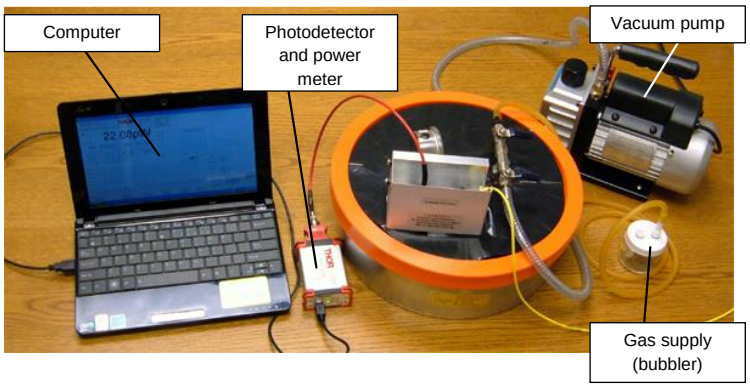

Figure 7. Photograph of the experimental setup to investigate RE phosphor based films for chemical sensing with the major components of the Analyzer AOR-001X.

Figure 8. Top view of analyzer AOR-002EX with open cover.

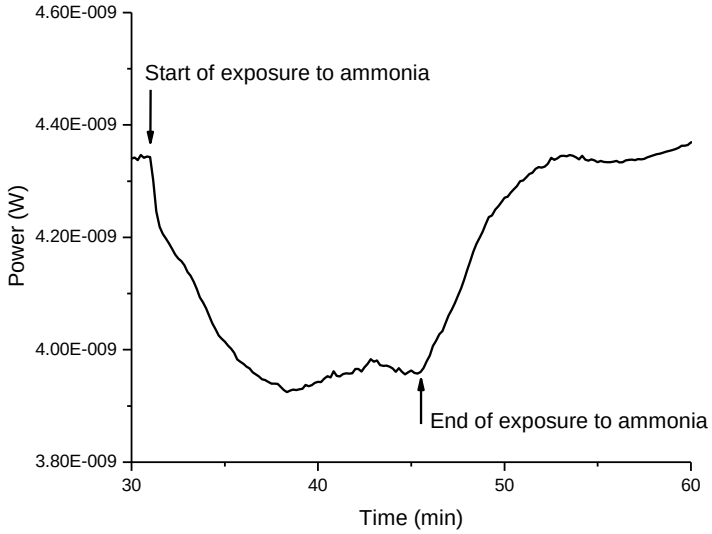

Figure 9. Time plot of the response of the sample nano-composite RE based reagent film to the exposure to 5% ammonia in air.

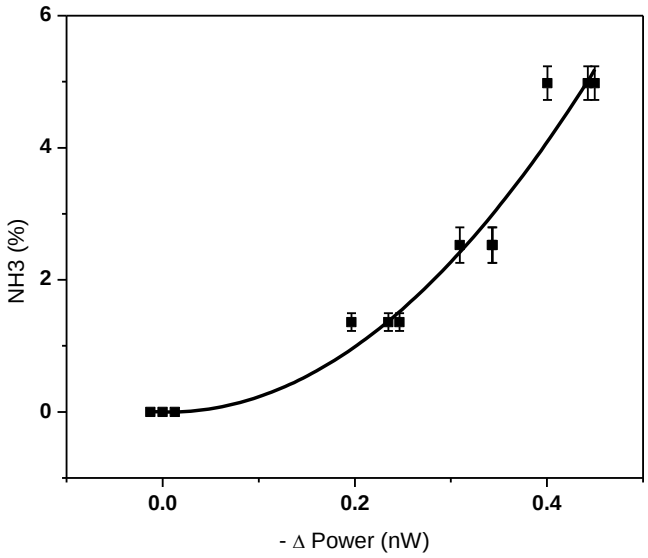

Figure 10. Ammonia concentration plotted versus the sensor output. Solid line presents the approximation quadratic calibration curve.

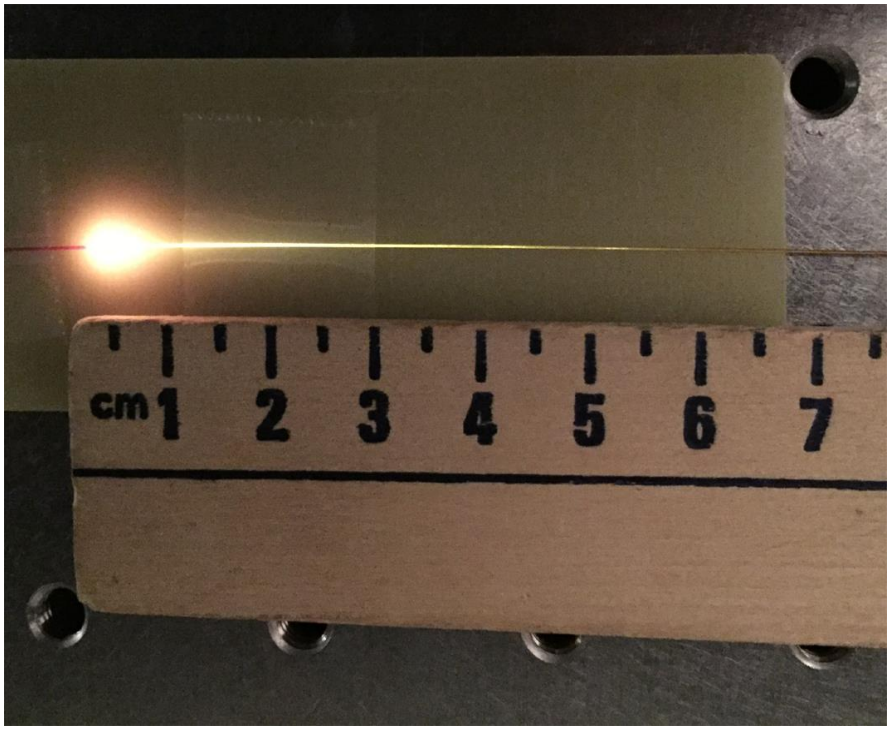

Figure 11. Image of the nanocolloid optical fiber amplifier based on a hollow fiber filled with the nanocolloid of RE phosphor $NaYF_4$: Yb^{3+}, Er^{3+} in a high-index liquid. The bright trace of visible light is produced by the upconversion emission from the nanocolloid pumped with a 980-nm IR radiation entering the fiber from the left. The pump radiation is delivered via a 980/1550-nm single-mode optical fiber spliced to the hollow fiber using Optical Fiber Splicer System including Fujikura 12S+CT-30 fusion splicer and LFS-004 (SSSOT) splicer/integrity tester.

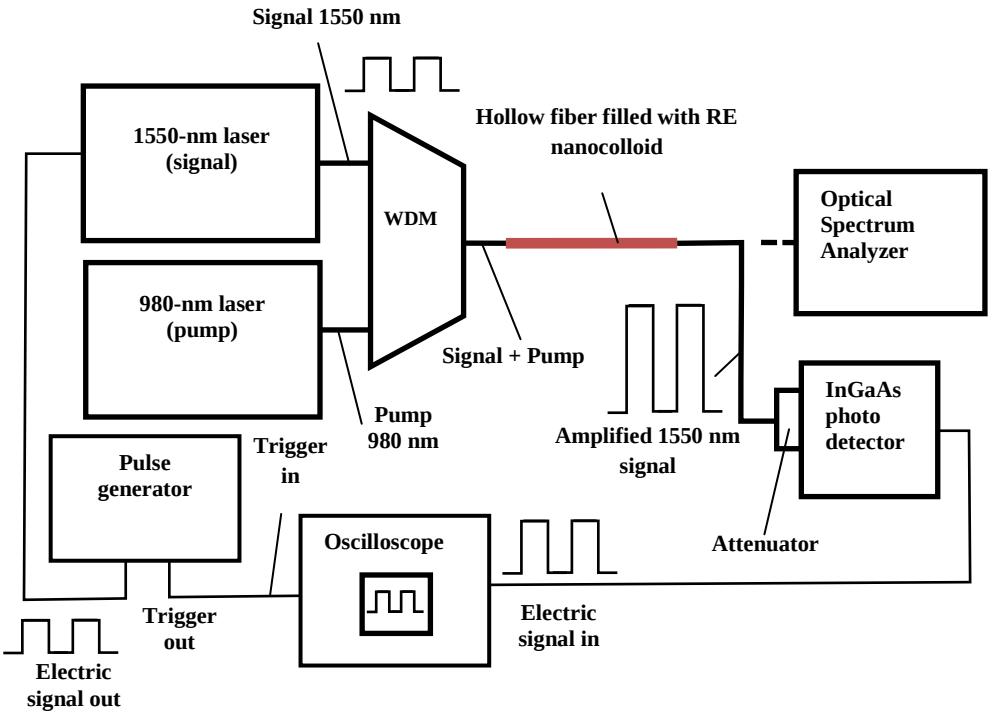

Figure 12. Experimental setup to characterize a nanocolloid fiber amplifier using Optical Fiber Spectrum Analyzer MS9740A (Anritsu) and Digital Pulse Generator DG53502 (Stanford Research).

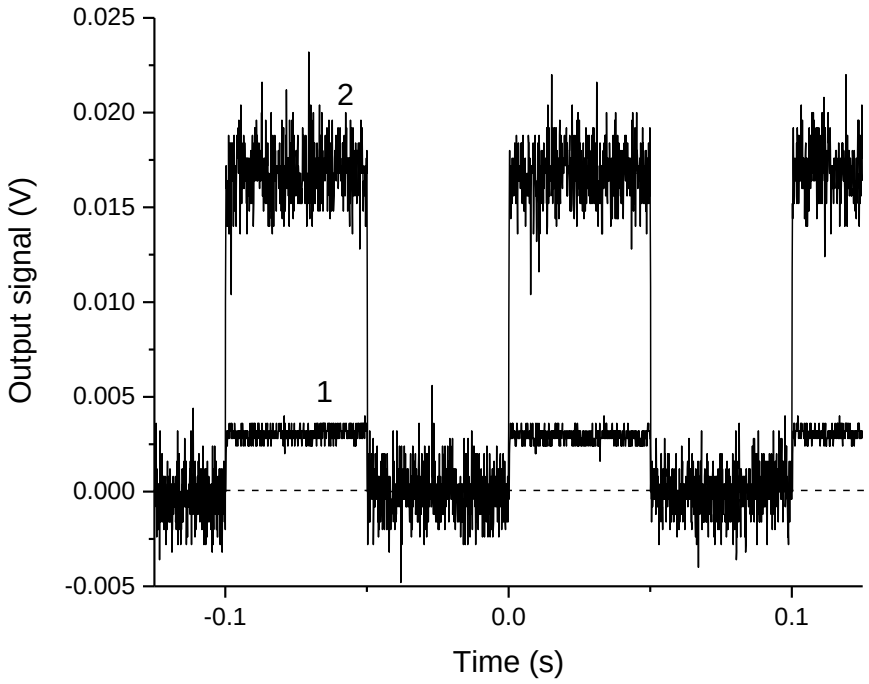

Figure 13. Output pulsed signal (1550 nm) for pump power: 0 mw (1) and 4.0 mW (2).

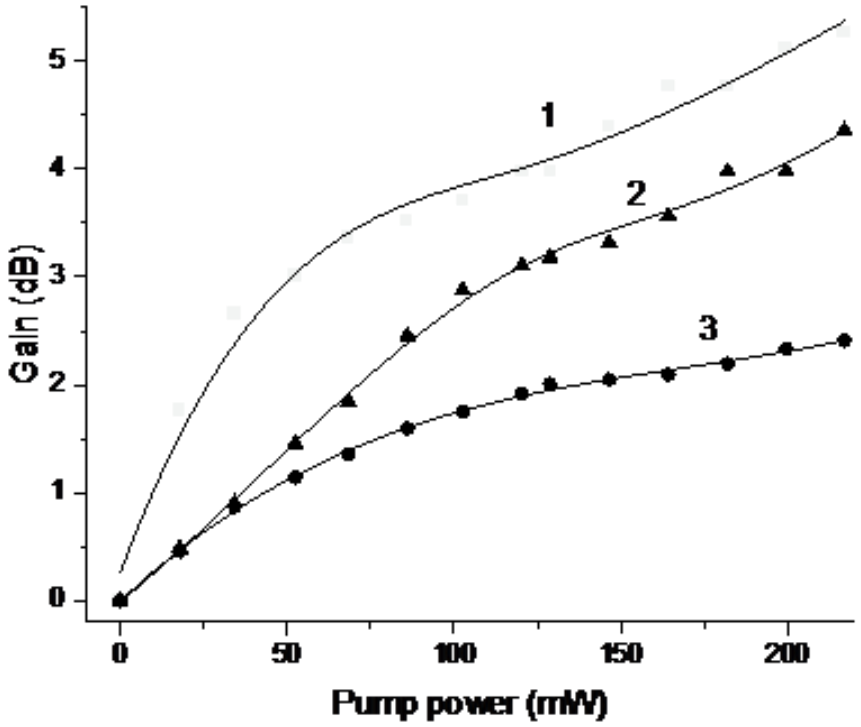

Figure 14. Gain versus pump power for input signal: 0.05 mW (1); 0.1 mW (2); 0.15 mW (3).

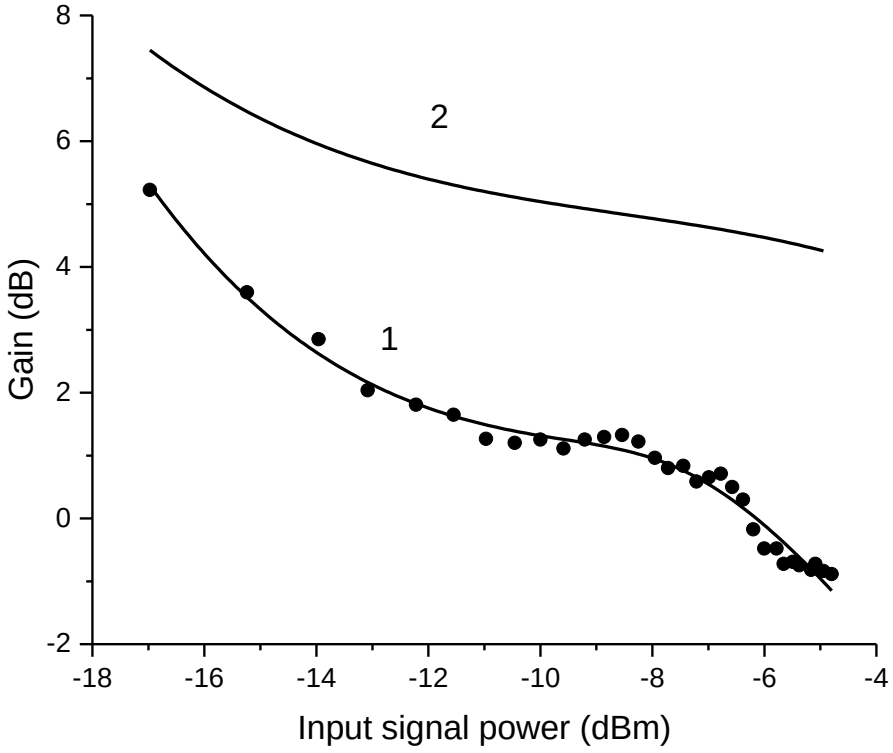

Figure 15. Gain versus input signal for pump power: 129 mW (1); 217 mW.

6. Student participants exposed to the acquired instrumentation

a) Ashley Lewis (Chemistry Major, Senior).
b) Ruben Valentine (Engineering Major, Senior)
c) Donald M. Wright III (Engineering Major, Senior)
d) Danielle Lewis (Engineering Major, Senior)
e) Marcus Valentine (Engineering Major, Senior)

7. Presentations and paper/patent applications submitted/published

Presentations

Poster presentation was presented by the PI and his student in San Francisco, CA, in Feb. 2014 at Photonics West 2014.
Poster presentation was presented by the PI and his student in San Francisco, CA, in Feb. 2015 at Photonics West 2015.

Publications

1. Abdalla M. Darwish, Simeon Wilson, Sergey Sarkisov, Darayas Patel, "Double pulse laser deposition of polymer nanocomposite $NaYF_4$:Tm^{3+}, Yb^{3+} films for optical sensors and light emitting applications," in *Photonic Fiber and Crystal Devices: Advances in Materials and Innovations in Device Applications VII*, edited by Shinzhuo Yin, Ruyan Guo, Proc. of SPIE Vol. 8847(2014), 884702, 884702-1—88702-13.
2. Abdalla M. Darwish, Allan Burkett, Ashley Blackwell, Keylantra Taylor, Sergey Sarkisov, Darayas Patel, Brent Koplitz, and David Hui, Polymer-inorganic nano-composite thin film upconversion light emitters prepared by double-beam matrix assisted pulsed laser evaporation (DB-MAPLE) method, Composites Part B 68 (2015), 355–364.
3. Abdalla M Darwish, Simeon Wilson, Ashley Blackwell, Keylantra Taylor, Sergey Sarkisov, Darayas Patel, Brent Koplitz, and David Hui, New double-beam matrix assisted pulsed laser evaporation (DB-MAPLE) method for making polymer nano-composite coatings, Proceedings of ICCE-22, Twenty Second Annual International Conference on Composites or Nano-Engineering, Edited by David Hui, July 13-19, 2014, Malta, 2 pages.
4. Abdalla M. Darwish, Allan Burkett, Ashley Blackwell, Keylantra Taylor, Vernell Walker, Sergey Sarkisov, Brent Koplitz, "Efficient upconversion polymer-inorganic nanocomposite emitters prepared by the double beam matrix assisted pulsed laser evaporation (DB-MAPLE," in *Photonic Fiber and Crystal Devices: Advances in Materials and Innovations in Device Applications VIII*, edited by Shinzhuo Yin, Ruyan Guo, Proc. of SPIE Vol. 9200 (2014) 92000C, 92000C-1—92000C-15.
5. Darayas Patel, Ashley Lewis, Donald Wright III, Maucus Valentine, Danielle Lewis, Ruben Valentine, and Sergey Sarkisov, "Upconversion, size analysis, & fiber filling of $NaYF_4$: Ho^{3+}, Yb^{3+} crystals & nanocolloids" in *Optical Components and Materials XI*, edited by Michel J. F. Digonnet, Shibin Jiang, Proc. of SPIE Vol. 8982, 898221(2014) 898221-1 – 898221-6.
6. Darayas Patel, Ashley Lewis, Donald Wright III, Danielle Lewis, Ruben Valentine, Maucus Valentine, Dennis Wessley, Sergey Sarkisov, and Abdalla M. Darwish "Optical properties and size distribution of the nano-colloids made of rare-earth ion-doped $NaYF_4$" in *Optical*

Components and Materials XII, edited by Shibin Jiang, Michel J. F. Digonnet, Proc. of SPIE Vol. 9359, 93591L (2015) 93591L-1 – 93591L-9.

7. Abdalla M. Darwish, Simeon Wilson, Ashley Blackwell, Keylantra Taylor, Sergey S. Sarkisov, Darayas N. Patel, and Brent Koplitz, Ammonia Sensor based on polymer-inorganic nano-composite thin film upconversion light emitter prepared by double-beam pulsed laser deposition, American J. of Materials Sciences 5(3A) (2015), 8-15.
8. Abdalla M. Darwish, Simeon Wilson, Ashley Blackwell, Keylantra Taylor, Sergey Sarkisov, Darayas Patel, Paolo Mele, Michael W. Johnson, Xiaodong Zhang, and Brent Koplitz, "Polymer-inorganic nanocomposite thin film emitters, optoelectronic chemical sensors, and energy harvesters produced by multiple-beam pulsed laser deposition," in *Photonic Fiber and Crystal Devices: Advances in Materials and Innovations in Device Applications IX*, edited by Shizhuo Yin, Ruyan Guo, Proc. of SPIE Vol. 9586 (2015) 958602, 14 pages.
9. Abdalla M. Darwish, Simeon Wilson, Ashley Blackwell, Keylantra Taylor, Sergey Sarkisov, Darayas Patel, Paolo Mele, and Brent Koplitz, "Multi-beam pulsed laser deposition: new method of making nanocomposite coatings," in *Photonic Fiber and Crystal Devices: Advances in Materials and Innovations in Device Applications IX*, edited by Shizhuo Yin, Ruyan Guo, Proc. of SPIE Vol. 9586 (2015) 958605, 13 pages.

Submitted for publication

Abdalla Darwish, Abdul Aziz Muhammad, Deonte Alexander, Sergey Sarkisov, Darayas Patel, Paolo Mele, Brent Koplitz, Michael Johnson, Xiaodong Zhang, Polymer nano-composite films with inorganic upconversion phosphor and electro-optic additives made by concurrent triple-beam matrix assisted and direct pulsed laser deposition, submitted to Composites Part B.